Triggering Mechanisms for Transport Barriers

O. Dumbrajs[2], J. Heikkinen[1], S. Karttunen[1], T. Kiviniemi[2], T. Kurki-Suonio[2], M. Mantsinen[2], K. Rantamäki[1], S. Saarelma[2], R. Salomaa[2], S. Sipilä[2], T. Tala[1]

Euratom-TEKES Association
[1] VTT Chemical Technology, P.O. Box 1404, FIN-02044 VTT, Finland
[2] Helsinki University of Technology, P.O. Box 2200, FIN-02015 HUT, Finland

e-mail contact of main author: Jukka.Heikkinen@vtt.fi

Abstract. The radial shear $w_{E\times B}$ of the $E\times B$ flow is evaluated with the Monte Carlo orbit following code ASCOT at the onset of the L-H transition and internal transport barriers (ITB) in JET, TFTR, ASDEX Upgrade, TEXTOR, and FT-2 tokamaks. Systematically, a large shear (sufficient for turbulence suppression) is found for local parameters close to the experimental threshold conditions at the barrier location. For L-H transition in JET and ASDEX Upgrade, the large shear is obtained by increasing the edge ion temperature. For TEXTOR, the radial electric field and the electrode current bifurcate at a threshold electrode voltage. In a JET database study, toroidal rotation is found to be dominant in triggering the JET ITB, and an empirical s-$w_{E\times B}$ fit is found for the transition threshold. For TFTR and FT-2, in which toroidal rotation does not play a role, ASCOT predicts a significant $w_{E\times B}$ shear for the ITB conditions. The ripple-induced transport is not found to be important here.

1. Introduction

In strongly heated plasmas where anomalous transport driven by microturbulence degrades the plasma confinement, transport barriers are observed to appear in regions with strong rotation/electric field shear. Indeed, the magnetic shear and the shear in the radial electric field E_r (and in the associated poloidal rotation) can define the confinement properties of a discharge. Qualitatively different regimes of enhanced confinement have been observed, including, e.g., H-mode and ITBs. The E_r field can be evaluated from the force balance

$$E_r = (1/Zen)dp/dr + u_f B_q - u_q B_f \,, \qquad (1)$$

where u_f (u_q) is the toroidal (poloidal) component of the ion velocity, e is the electron charge, Z is the ion charge number, n is the ion density, and p is the ion pressure. The poloidal (toroidal) component of the magnetic field is B_q (B_f), and r is the minor radius (half-width). Identifying experimentally the mechanism behind the generation of a strongly sheared E_r field is hindered by the difficulty of accurate measurements of p, u_f, and u_q close to the barrier.

We investigate the role of the magnetic shear s and the shearing rate $w_{E\times B}$ of the $E\times B$ flow across a transport barrier for various confinement regimes. We also simulate the generation of E_r for a wide variety of tokamaks ranging from the tiny FT-2 tokamak (a = 8 cm, R = 55 cm) to JET. A close examination of the ITB formation in the JET optimised shear experiments reveals an empirical s-$w_{E\times B}$ fit for the transition threshold. The u_f -term overwhelmingly dominates in Eq. (1), so that no additional triggering mechanism for the transition is needed. For other experiments, in which u_f can not play a significant role, the dynamics of E_r and its possible bifurcation are obtained from a self-consistent, fully kinetic 5D neoclassical simulation of the radial current balance.

We simulate the various tokamak experiments using the guiding-centre orbit following Monte Carlo code ASCOT, which finds the ion fluxes and solves the polarisation equation for E_r in

radius and time [1]. ASCOT [2] can use real tokamak magnetic background data (including wall and divertor structures) from experiment databases, and it uses the MPI (Message Passing Interface) standard to facilitate massively parallel computation for large test particle ensembles. An energy- and momentum-conserving binary collision model is included. The code has been benchmarked against the known neoclassical expressions of transport fluxes, parallel viscosity, and relaxation rate of poloidal rotation for poloidal Mach numbers [3] extending well into the supersonic region. We follow the guiding centre orbits in real tokamak geometries, taking into account the orbit loss of both thermal and tail ions. The lost ions can be re-initialised at the separatrix in a way that simulates the replacement of the lost charge. The perpendicular viscosity drift is added to the ion motion, but it has importance only for very high shear. Leaving out all ambipolar processes, such as ion flux due to electron collisions and anomalous transport (which we assume ambipolar), E_r can be solved from the ion fluxes using the polarisation equation. The simulation is continued until the electric field balances the current components. Biased edge probe experiments can be simulated by including the electrode current I_E and neutral charge exchange damping in the polarisation equation.

In this work, with the ASCOT code, (1) the L-H transition threshold is explored in ASDEX Upgrade and JET configurations; (2) the formation of an ITB is investigated for the FT-2 and TFTR tokamaks in which an ITB is observed to occur without a net source of toroidal momentum; and (3) the biased edge probe experiments at TEXTOR are simulated. Investigating the JET database interpretatively using the JETTO code, an empirical s-$w_{E'B}$ fit for the formation of the transport barrier is obtained.

2. L-H Transition in ASDEX Upgrade and JET, Induced Transition in TEXTOR

In an L-H transition, a strong negative E_r is observed to appear in the plasma edge, creating a transport barrier there. In a series of ASCOT simulations we investigate the dependence of the steady-state E_r on the background parameters (edge density, temperature, toroidal magnetic field, and plasma current). No spontaneous bifurcation in E_r is found (even in the banana limit), i.e. no multiple solutions exist, but the field changes follow the changes in the plasma parameters as shown in Fig. 1(a). When compared to an empirical criterion for the critical shear [4], the obtained orbit loss driven E_r shear is found high enough for turbulence suppression. Indeed, the dependence of the critical shear on the background parameters is similar [1] to that found for a transition in ASDEX Upgrade experiments [5].

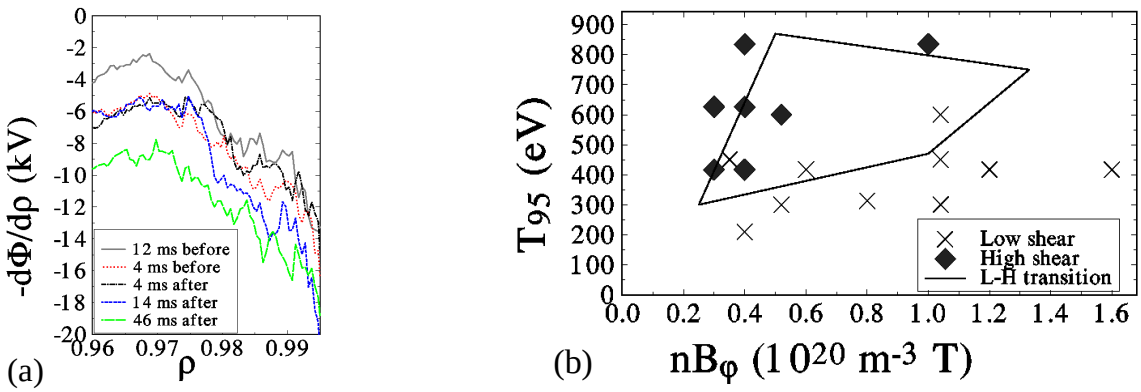

FIG. 1. (a) -dF /dr μ E_r as a function of r using experimental density and temperature data across the transition in ASDEX Upgrade. (b) Observed (T_{95} ,nB_f) region at L-H transition in JET (bounded area), and the low and high shear results from ASCOT simulations (crosses and diamonds).

Figure 1(b) shows the cases simulated for JET as a function of edge temperature T_{95} and the product of the line-averaged density and magnetic field. The obtained $w_{E'B}$ shear is classified as *high* or *low* according to whether it exceeds an empirical criterion 5×10^5 s^{-1} for the critical shear within a turbulence decorrelation length (~ 1-2 cm) from the separatrix or not. In ASCOT simulations, the region where the critical shear is exceeded coincides well with the experimental parameter regime for an L-H transition (roughly indicated by the quadrangle). Although no bifurcation is found for a spontaneous transition either in ASDEX Upgrade or JET, when simulating the electrode polarisation in TEXTOR configuration we obtain a bifurcation in E_r and make the first numerical observation of a soliton-structured E_r [1].

3. Formation of an ITB in JET, TFTR, and FT-2

(a) ITB formation in JET. A thermal barrier can also be formed in the interior of a tokamak plasma. A weak or negative magnetic shear facilitates the formation of such a barrier. We investigate the threshold conditions for an ITB in JET by evaluating E_r from Eq. (1). In Fig. 2, E_r and its different components are presented (a) 0.6 s before the onset of the ITB and (b) 0.6 s after the ITB formation for the JET optimized shear (OS) discharge No. 46664. All variables in Eq. (1) have their measured values except $u_{\theta,}$ which is assumed neoclassical. The contribution from the neutral beam-driven toroidal rotation (dash-dotted curve) is clearly dominant in the total E_r (thick solid curve) both before and after the ITB formation. The dominance of $E_{r,f}$ is particularly pronounced in this discharge because the poloidal velocity term $E_{r,q} = u_q B_f$ (dotted curve) almost cancels the pressure gradient term $E_{r,p} = (1/Zen)dp/dr$ (dashed curve). In Fig. 2(b), the footpoint of the ITB is at r = 0.56. The values and behaviour of E_r are similar also for other JET OS discharges.

We calculate the $w_{E'B}$ shearing rate from [6]

$$w_{E\times B} = \left| \frac{RB_q^2}{B_f} \frac{\partial}{\partial \Psi} \frac{E_r}{RB_q} \right|, \qquad (2)$$

where Ψ is the poloidal flux, R is the major radius, and E_r is calculated from Eq. (1). In Fig. 3,

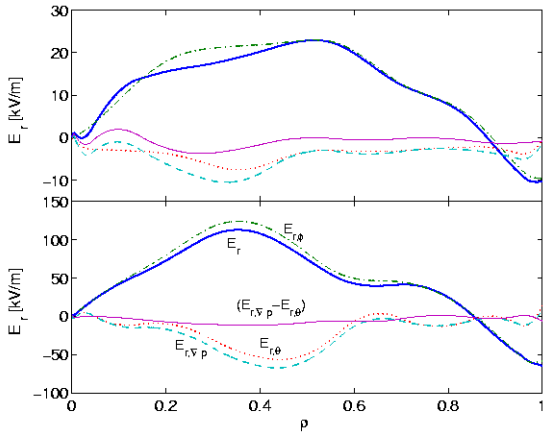

FIG. 2. E_r and its components in JET (a) 0.6 s before and (b) 0.6 s after the ITB formation.

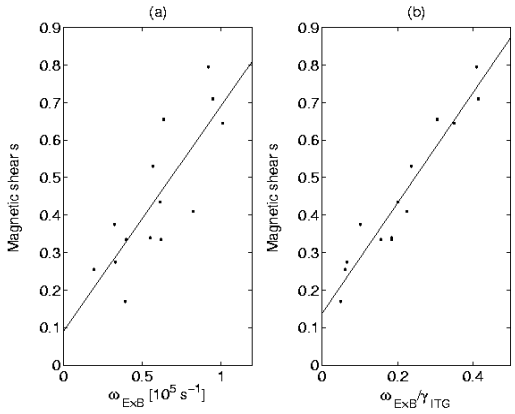

FIG. 3. Magnetic shear versus (a) $w_{E'B}$ and (b) $w_{E'B}$ /g_{ITG} at ITB location for the threshold conditions. The straight lines are best fits calculated with the least-squares method.

we show the shear quantities s and $w_{E'B}$ for a number of JET ITB pulses. Both are evaluated at the barrier location at the onset of the barrier (within the experimental accuracy). The points were obtained from both L-mode and ELMy H-mode pulses and, consequently, the parameter range of the pulses is wide: B_f varies between 1.8 T and 4.0 T, the input power in the range 10-30 MW, and the diamagnetic energy in the range 3-12 MJ. We have used the JETTO transport code to calculate the magnetic shear, and g_{ITG} denotes the linear growth rate of the Ion Temperature Gradient (ITG) turbulence. The estimated regression line takes the form $s = 0.60 w_{E'B} + 0.091$ (scaled by 10^5) in Fig. 3(a), and $s = 1.5 w_{E'B}/g_{ITG} + 0.14$ in Fig. 3(b).

The threshold for ITB formation in the s-$w_{E'B}/g_{ITG}$ space can be interpreted as follows: the $w_{E'B}$ flow shear must be large enough to suppress the turbulence arising from the combined effect of the ITG turbulence (growth rate g_{ITG}) and the magnetic shear (s). Consequently, an ITB can exist only below the line in Fig. 3(b). When the line is crossed, an ITB is either formed or collapses, depending on the direction of the crossing. In both L-mode and ELMy H-mode pulses, all plasmas covering a wide range in B_f, P_{in} and W_{dia} are found to obey this rule. Even the three ITB back-transitions included in the analysis fit the same straight line.

(b) Can the ripple transport trigger an ITB? It has been suggested [7] that the particle flux induced by toroidal field ripple can drive E_r to bifurcate over the local maximum of the poloidal viscosity. This mechanism appears consistent with the sudden jump in E_r observed in TFTR [8] just prior to the onset of the enhanced reversed shear (ERS) mode. The process is purely neoclassical and thus ideal for testing with ASCOT. We simulate the ITB formation region (r = 0.2…0.4 m) in TFTR-like configuration using parameters given in Ref. [8]: ripple value d = 0.013, u_f = 0, and a large temperature gradient, $dT/dr \approx$ 70 keV/m^2. Indeed, E_r is found to deviate substantially from its modest, ambipolar values dictated by the plasma profiles (see Fig. 4). However, the sheared electric fields are obtained also in the *absence* of a magnetic ripple. Even increasing the ripple strength to ten times its nominal value brings only slight modifications to the E_r profile. Consequently, no evidence of a ripple-induced confinement transition has been found, but our study indicates that as the gradient length L_T approaches the orbit width D_b (here $L_T, D_b \approx$ 10 cm), the emerging radial electric field can significantly deviate from its ambipolar value.

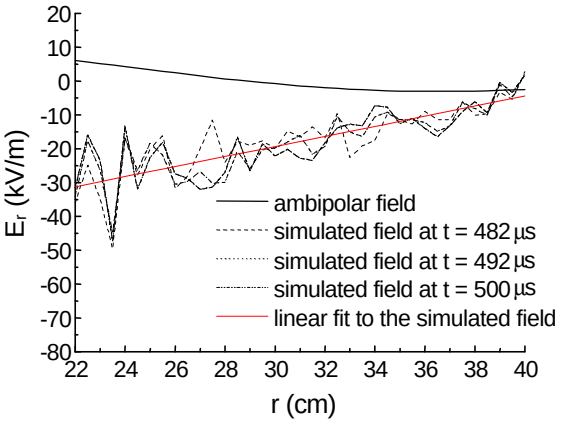

FIG. 4. The simulated neoclassical E_r field for the ITB region in TFTR-like configuration. Also shown is the pure ambipolar field calculated analytically from the plasma profiles.

(c) $w_{E'B}$ shear in a small, low current tokamak. On FT-2 tokamak, in the presence of LH heating, the plasma confinement has been observed to improve [9]. Sometimes the transport barrier is found to form near the plasma edge, while other discharges show evidence for an ITB formation. ASCOT simulations that cover the entire plasma cross section indicate that, indeed, for strong enough gradients, as shown in Figs. 5(a) and 5(b), a distinct well structure for E_r forms in the interior of the FT-2 plasma, see Figs. 5(c) and 5(d). Because in these plasma conditions (B_T = 2.2 T, I_p = 22 kA) the gradient scale length can be smaller than the

orbit widths for $E_r = 0$, the mechanism is beyond standard neoclassical theory and does not yet have a full theoretical explanation. The resulting E_r shear is significantly larger than the neoclassical ambipolar estimate. It is of interest to note that the poloidal $E \times B$ rotation velocity for the threshold conditions in FT-2 well exceeds the thermal ion velocity. Thus the particle orbits become strongly squeezed and, consequently, the particles are better confined (neoclassically). In fact, small-radius configurations with low plasma current seem to be particularly amenable for high $w_{E \times B}$ shear and transport barrier formation, and thus may provide interesting possibilities for high performance, if also the MHD stability can be shown to improve together with the transport.

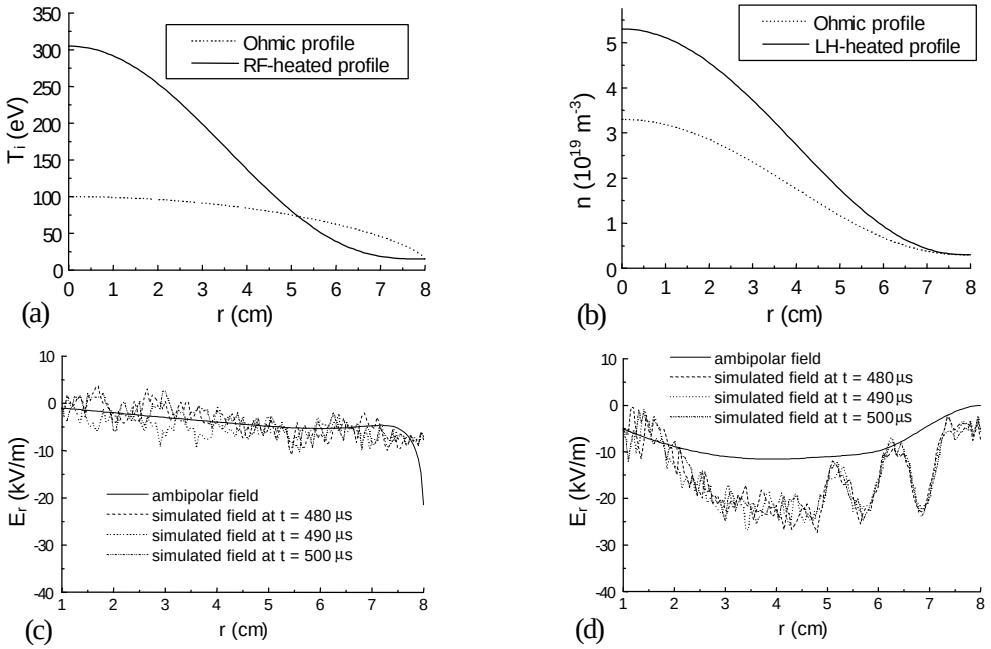

FIG. 5. Temperature (a) and density (b) profiles used in the FT-2 study. Simulated radial E_r profile during the last 30 ms for the Ohmic profiles (c) and RF-heated profiles (d).

4. Conclusions

For toroidal devices, the electric potential can be reliably evaluated with a Monte Carlo particle following code exploiting the radial current balance condition. Significant E_r shear is found from ASCOT simulations at onset conditions of transport barriers in various tokamaks. In a JET database study, toroidal rotation is found to be dominant in triggering the JET ITB, and an empirical s-$w_{E \times B}$ fit for the transition threshold is revealed.

[1] HEIKKINEN, J.A., KIVINIEMI, T.P., PEETERS, A.G., Phys. Rev. Lett. **84** (2000) 487.
[2] SIPILÄ, S.K., Monte Carlo Simulation of Charged Particle Orbits in the Presence of RF Waves in Tokamak Plasmas, DSc thesis, Helsinki University of Technology, Espoo (1997); available from http://www.hut.fi/Units/AES/ascot.htm
[3] KIVINIEMI, T.P., HEIKKINEN, J.A., PEETERS, A., Nucl. Fusion **40** (2000) 1587.
[4] GOHIL, P., BURRELL, K.H., CARLSTROM, T.N., Nuclear Fusion **38** (1998) 93.
[5] SUTTROP, W., et al., Plasma Phys. Control. Fusion **39** (1997) 2051.
[6] HAHM, T.S., BURRELL, K.H., Phys. Plasmas **2** (1995) 1648.
[7] SHAING, K.C., et al., Phys. Rev. Lett. **83** (1999) 3840.
[8] BELL, R.E., et al., Phys. Rev. Lett. **81** (1998) 1429.
[9] LASHKUL, S.I., et al., Europhys. Conf. Abstr. **23J** (1999) 1729.